ARTICLES

Journal of Semiconductors
(2020) 41, 082002
doi: 10.1088/1674-4926/41/8/082002

High-performance junction field-effect transistor based on black phosphorus/β-Ga_2O_3 heterostructure

Chang Li[1, 2], Cheng Chen[2, 3], Jie Chen[2, 3], Tao He[4], Hongwei Li[2, 5], Zeyuan Yang[1, 2], Liu Xie[2], Zhongchang Wang[6], and Kai Zhang[2, †]

[1]Nano Science and Technology Institute, University of Science and Technology of China, Suzhou 215123, China

[2]*i*-Lab, Suzhou Institute of Nano-Tech and Nano-Bionics (SINANO), Chinese Academy of Sciences, Suzhou 215123, China

[3]School of Materials Science and Engineering, Shanghai University, Shanghai 200444, China

[4]CAS Key Laboratory of Nanodevices and Applications, Suzhou Institute of Nano-Tech and Nano-Bionics (SINANO), Chinese Academy of Sciences, Suzhou 215123, China

[5]Institute of Microscale Optoelectronics, Collaborative Innovation Centre for Optoelectronic Science & Technology, Key Laboratory of Optoelectronic Devices and Systems of Ministry of Education and Guangdong Province, College of Physics and Optoelectronic Engineering, Shenzhen Key Laboratory of Micro-Nano Photonic Information Technology, Guangdong Laboratory of Artificial Intelligence and Digital Economy (SZ), Shenzhen University, Shenzhen 518060, China

[6]International Iberian Nanotechnology Laboratory (INL), Avenida Mestre José Veiga s/n, Braga 4715-330, Portugal

Abstract: Black phosphorous (BP), an excellent two-dimensional (2D) monoelemental layered p-type semiconductor material with high carrier mobility and thickness-dependent tunable direct bandgap structure, has been widely applied in various devices. As the essential building blocks for modern electronic and optoelectronic devices, high quality PN junctions based on semiconductors have attracted widespread attention. Herein, we report a junction field-effect transistor (JFET) by integrating narrow-gap p-type BP and ultra-wide gap n-type β-Ga_2O_3 nanoflakes for the first time. BP and β-Ga_2O_3 form a vertical van der Waals (vdW) heterostructure by mechanically exfoliated method. The BP/β-Ga_2O_3 vdW heterostructure exhibits remarkable PN diode rectifying characteristics with a high rectifying ratio about 10^7 and a low reverse current around pA. More interestingly, by using the BP as the gate and β-Ga_2O_3 as the channel, the BP/β-Ga_2O_3 JFET devices demonstrate excellent n-channel JFET characteristics with the on/off ratio as high as 10^7, gate leakage current around as low as pA, maximum transconductance (g_m) up to 25.3 μS and saturation drain current (I_{DSS}) of 16.5 μA/μm. Moreover, it has a pinch-off voltage of –20 V and a minimum subthreshold swing of 260 mV/dec. These excellent n-channel JFET characteristics will expand the application of BP in future nanoelectronic devices.

Key words: two-dimensional semiconductor; black phosphorous; β-gallium oxide; vdWs heterostructure; junction field-effect transistor

Citation: C Li, C Chen, J Chen, T He, H W Li, Z Y Yang, L Xie, Z C Wang, and K Zhang, High-performance junction field-effect transistor based on black phosphorus/β-Ga_2O_3 heterostructure[J]. *J. Semicond.*, 2020, 41(8), 082002. http://doi.org/10.1088/1674-4926/41/8/082002

1. Introduction

As an emerging material with an ultra-wide bandgap (4.9 eV) at room temperature, high theoretical critical field strength (8 MV/cm), superior power switching capability and large Baliga's figure of merit, β-gallium oxide (β-Ga_2O_3) has been considered a competitive material for the next generation of high power electronic and optoelectronic devices. The unintentionally doped β-Ga_2O_3 exhibits inherent n-type conductivity because the oxygen vacancy acts as a donor[1–5]. Until now, the epitaxially grown β-Ga_2O_3 thin films and single-crystalline β-Ga_2O_3 wafers were successfully obtained for fabricating various metal–oxide–semiconductor field-effect transistors (MOSFETs)[4–7]. Nevertheless, the performances of MOSFETs are severely influenced by oxide dielectrics. Charge transport will be suppressed due to the poor-quality dielectric surface[8]. Alternatively, as an important part of field-effect transistors (FETs), junction field-effect transistors (JFETs) have a simple device structure without dielectric layers. The working mechanism of JFETs is controlling the depletion region in the semiconducting channel with a reverse biased PN junction[9]. In detail, it is controlling the source–drain current (I_{ds}) by the gate–source voltage (V_{gs}). For n-channel JFET, the conductive channel became narrow with V_{gs} decreased, resulting in the channel resistance increasing and the I_{ds} decreasing. When V_{gs} up to pinch-off voltage, the channel will be fully depleted, resulting in the JFET being switched off. Unlike MOSFETs, β-Ga_2O_3 is rarely applied to JFETs due to the difficulty of effective hole doping for n-type β-Ga_2O_3[10].

Recently, Barman *et al.* proved the single-crystalline β-Ga_2O_3 can be exfoliated into nanoflakes along the (100) plane direction while maintaining the superior properties of bulk crystals, even though it's not a layered 2D material bound together through the van der Waals (vdW) force[11]. As a quasi-

Correspondence to: K Zhang, kzhang2015@sinano.ac.cn
Received 29 MAY 2020; Revised 16 JUNE 2020.
©2020 Chinese Institute of Electronics

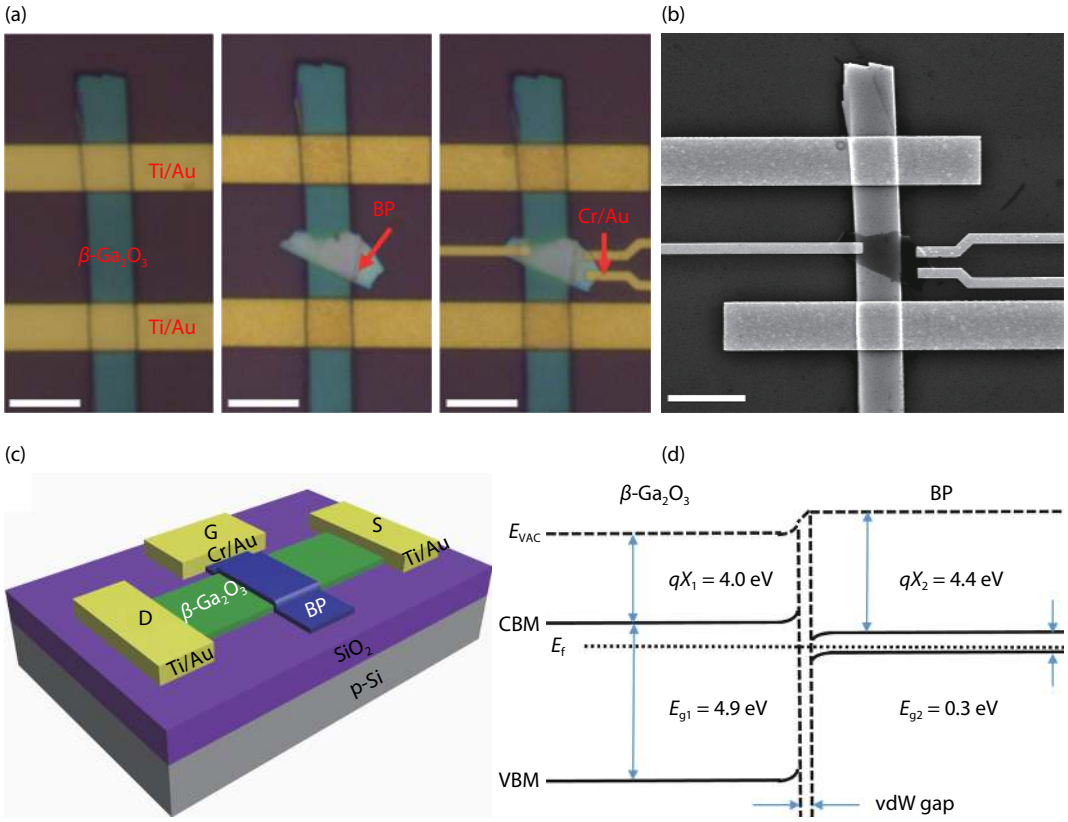

Fig. 1. (Color online) (a) Optical microscope images of fabrication steps of BP/β-Ga_2O_3 heterojunction device. The channel length and width of the β-Ga_2O_3 were 16 and 6 μm, respectively. (b) SEM image of an as-fabricated BP/β-Ga_2O_3 heterojunction device. (c) Schematic illustration of the JFET device fabricated on a Si/SiO_2 (285 nm) substrate. (d) Energy band diagram of multilayer p-type BP and n-type β-Ga_2O_3 heterojunctions with a vdW gap. Scale bars are 10 μm.

2D material, exfoliated β-Ga_2O_3 flakes had formed vdW heterojunctions by integrating with various 2D materials without lattice matching[12]. For example, β-Ga_2O_3/graphene vertical vdW heterostructure with a high breakdown electric field[13], double graphene-gate β-Ga_2O_3 metal–semiconductor FETs (MESFETs) for a logic inverter[14], β-Ga_2O_3/hexagonal boron nitride (h-BN) metal–insulator–semiconductor FET (MISFETs) with superior performances[15], etc. And more notably, Kim *et al.*reportedthatatypicalJFETstructurewithalow-dimensionalheterojunction PN diode. It was formed between mechanically exfoliated p-type WSe_2 and n-type β-Ga_2O_3[8]. This approach provides one way to fabricate JFETs based on β-Ga_2O_3 and achieve a high on/off ratio. However, due to the limitation of intrinsic properties of WSe_2, the integral performances of JFET based on β-Ga_2O_3/2D materials still need to improve.

As a novel 2D layered semiconductor material, black phosphorous (BP) is gradually receiving considerable attention, because it possesses a tunable direct bandgap (0.3 to 1.5 eV) by thickness (bulk to monolayer), high carrier mobility over 1000 $cm^2V^{-1}s^{-1}$, strong light-matter coupling, excellent intrinsic in-plane anisotropy and exciting biocompatibility[16–23]. Therefore, BP demonstrated remarkable performance in versatile applications, such as broadband photodetection[24–26], solar cells[27–30], biomedicine[31–34], logic circuit[35–38], catalysts[39, 40]. Moreover, BP shows the p-type intrinsic conduction although most 2D semiconductors are n-type because of inherent structural defects and strong electron doping from interfacial charge impurities[41]. Actually, the p-type materials are essential for forming PN heterojunctions which apply to electronic and optoelectronic devices. A variety of PN heterojunctions were produced between BP and other n-type materials, such as ZnO[37], MoS_2[42], InSe[43].

In this work, we demonstrate a vdW heterojunction JFET based on BP and β-Ga_2O_3. The mechanically exfoliated multilayer BP flakes as the gate and multilayer β-Ga_2O_3 flakes as the channel. The BP/β-Ga_2O_3 PN junction exhibits preeminent rectification characteristics with rectifying ratio higher than 10^7 and the reverse current as low as pA. The BP/β-Ga_2O_3 JFETs show excellent n-channel JFET characteristics with high on/off ratio about ~10^7, low gate leakage current around pA, high g_m of 25.3 μS and I_{DSS} of 16.5 μA/μm. Moreover, it has a pinch-off voltage of –20 V and a minimum subthreshold swing of 260 mV/dec. Additionally, the electrical performances of the BP/β-Ga_2O_3 JFET device at different temperatures are also discussed. This work not only expands the applications of BP in future nanoelectronic devices but also paves the way for vdW heterojunctions based on 2D semiconductors applying to realize high performance JFET devices.

2. Experiments

Material Characterizations: All nanoflakes were measured for thickness information and surface morphology through an atomic force microscope (AFM, Bruker Dimension ICON). Raman measurements were conducted in a micro-Raman system (LABRAM HR) with visible laser light (λ = 532 nm). The morphology and elemental mapping of the heterojunction were observed by scanning electron microscope (SEM, Quanta FEG 250).

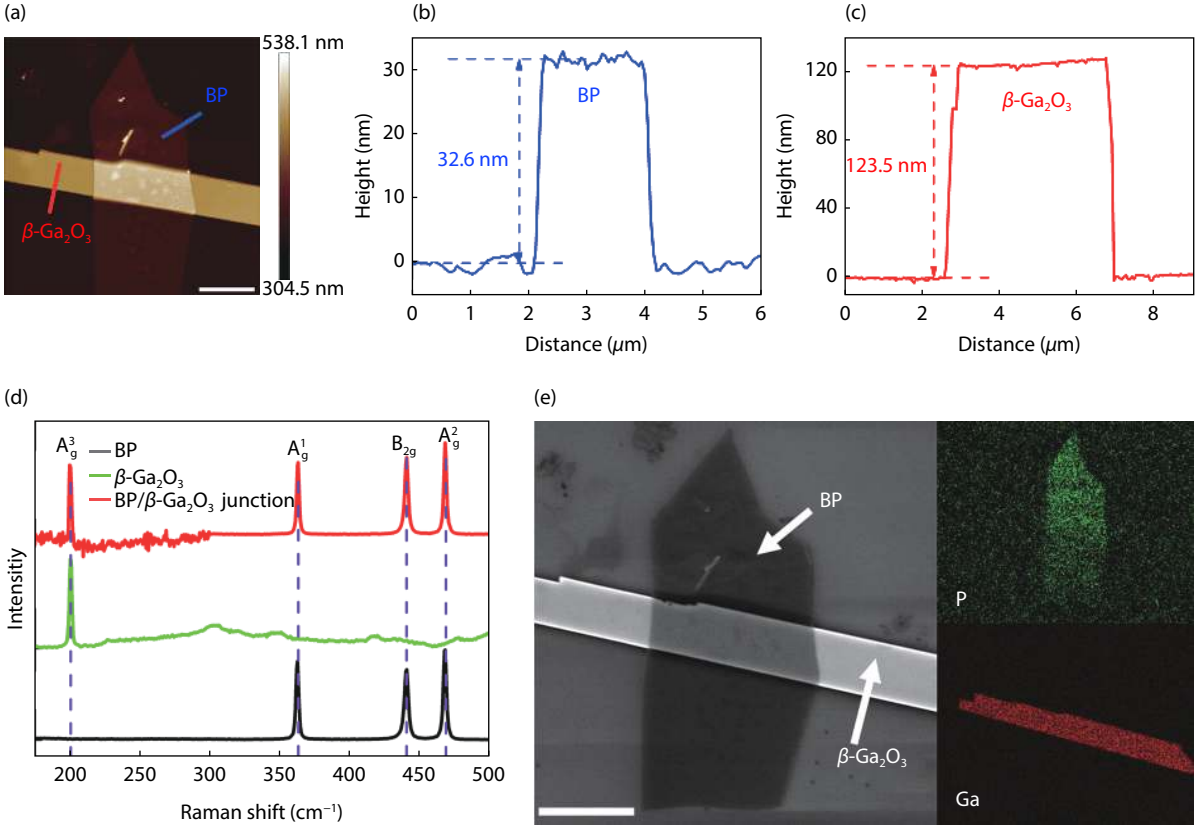

Fig. 2. (Color online) (a) AFM image of the BP/β-Ga_2O_3 heterojunction. (b, c) Height profiles of the exfoliated BP and β-Ga_2O_3 flakes in (a). The thicknesses of the nanoflakes are 32.6 and 123.5 nm, respectively. (d) Raman spectra of the BP, β-Ga_2O_3 and the BP/β-Ga_2O_3 overlapped regions obtained under a 532 nm laser. The black and green curve demonstrated typical multilayer BP flake and β-Ga_2O_3 flake. The red curve shows the peaks of the overlapped region. (e) SEM image of the BP/β-Ga_2O_3 heterostructure device (left) and corresponding EDS element mappings for Ga and P (right). Scale bars are 5 μm.

Device Fabrication: Using traditional dry transfer technology, the BP/β-Ga_2O_3 heterojunction was fabricated inside a glove box. First, β-Ga_2O_3 flakes were prepared from a bulk single-crystalline (100) β-Ga_2O_3 through the conventional mechanical exfoliation method and transferred onto Si/SiO_2 (285 nm) substrates. In order to remove the organic impurity, the substrates with β-Ga_2O_3 flakes were soaked into acetone for several hours before the device fabrication. Then, the source–drain electrodes of Ti/Au (30/120 nm) were fabricated using electron-beam lithography (JEOL JBX 5500) to define patterns, electron beam evaporator (ULVAC Ei-5Z) to deposit metal films and lift-off process. In order to achieve ohmic contact, rapid thermal annealing was carried out for 60 s at 475 °C in a nitrogen ambient. Afterwards, using the same way, few-layer BP flakes were separated from bulk BP crystals synthesized by mineralizer-assisted gas-phase transformation method. The exfoliated BP flakes were precisely transferred onto β-Ga_2O_3 through a picking-up and dropping process using the polydimethylsiloxane (PDMS) transfer technique. Finally, the contact metallization with BP was performed by depositing Cr/Au (10/70 nm) using the same method mentioned above. To avoid oxidation from O_2 and H_2O, the exposure time in ambient was limited within one hour during the fabrication process.

Electrical Characterizations: The electrical characteristics of the fabricated JFET were measured by a Sussmicrotec probe station with a Keithley 4200 semiconductor parameter analyzer.

3. Results and discussion

Fig. 1(a) shows the fabrication process of the BP/β-Ga_2O_3 heterojunction JFET device by using optical microscope images. Multilayer β-Ga_2O_3 flakes are prepared via mechanically exfoliation. BP/β-Ga_2O_3 heterojunctions are fabricated by the vdW force using an alignment dry transfer method (for more details, see Experiments). The quality of the as-fabricated BP/β-Ga_2O_3 heterojunction can be obtained from the SEM image (Fig. 1(b)). The surfaces of both BP and β-Ga_2O_3 materials were smooth and the heterojunction interface was clean. Fig. 1(c) shows schematic illustration of the BP/β-Ga_2O_3 heterojunction device on the Si/SiO_2 substrate. In this heterojunction device, the source–drain voltages (V_{ds}) is applied on β-Ga_2O_3, BP and Si/SiO_2 act as the gate and back gate, respectively. As shown in Fig. 1(d), the energy band diagram of BP/β-Ga_2O_3 heterojunction demonstrates the formation of a typical PN junction. According to the previous reports, the electron affinity (qX_1) and bandgap (E_{g1}) values of multilayer β-Ga_2O_3 are about 4.0 and 4.9 eV, respectively[6–8]. For multilayer BP, the electron affinity (qX_2) and bandgap (E_{g2}) values are about 4.4 and 0.3 eV, respectively[16–19]. The Fermi energy (E_f) of β-Ga_2O_3 almost close to conduction band minimum (CBM) but the E_f of BP close to valence band maximum (VBM), because multilayer β-Ga_2O_3 and multilayer BP are unintentional n-type and p-type doped, respectively. The heterojunction band diagram is extremely important to understand the operation mechanism of the heterojunction JFET device.

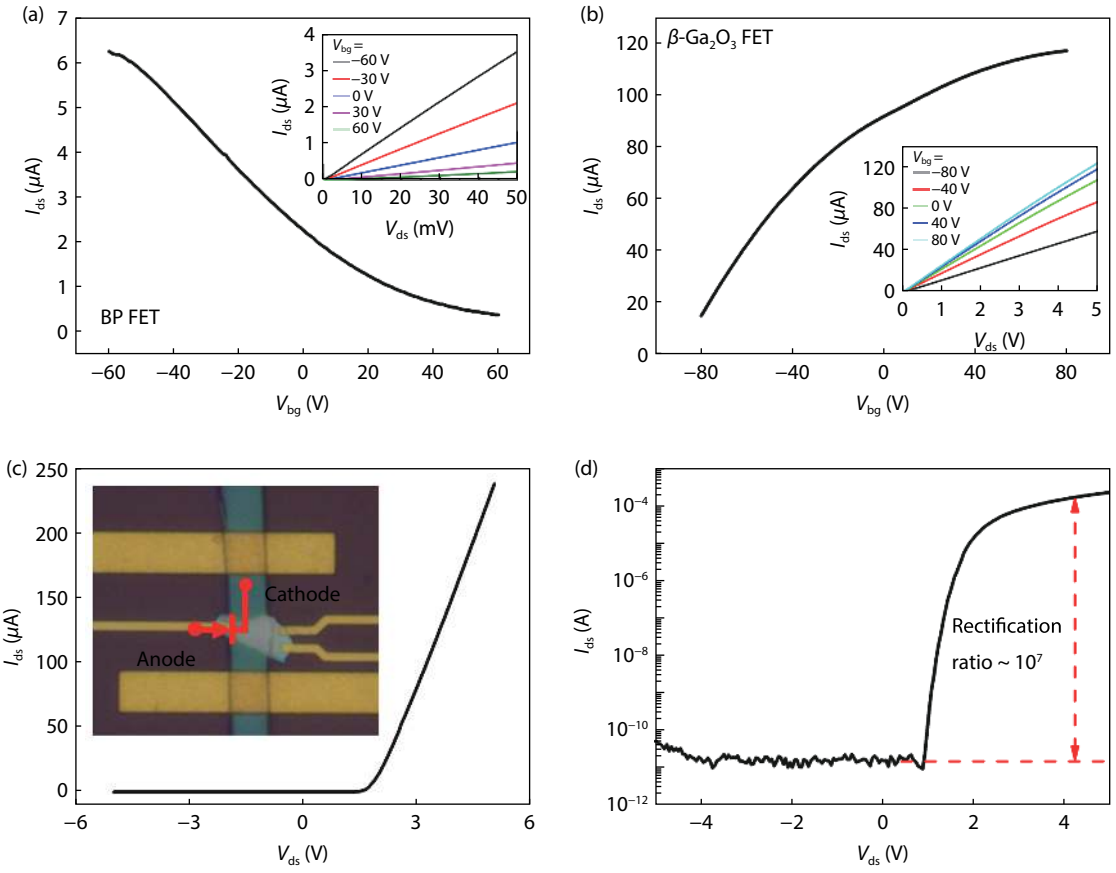

Fig. 3. (Color online) (a)Transfer characteristics for back-gate BP FET. Back gate voltage V_{bg} swept from –60 to 60 V with a fixed source–drain bias voltage V_{ds} = 0.1 V. (Inset: output characteristics for back gated BP FET. V_{bg} ranging from –60 to 60 V with steps of 30 V under V_{ds} swept from 0 to 50 mV.) (b) Transfer characteristics for back gate β-Ga_2O_3 FET. V_{bg} swept from –80 to 80 V with a fixed V_{ds} = 5 V (Inset: output characteristics for back-gate β-Ga_2O_3 FET. V_{bg} ranging from –80 to 80 V with steps of 40 V under V_{ds} swept from 0 to 5 V.) (c) I_{ds}–V_{ds} curve of BP/β-Ga_2O_3 PN heterojunction. It shows a typical rectifying behavior. (Inset: the circuit schematic diagram of the PN heterojunction.) (d) I_{ds}–V_{ds} semi-log plot of the BP/β-Ga_2O_3 PN heterojunction.

In order to obtain the thickness and surface morphology of the BP/β-Ga_2O_3 heterojunction, the AFM image and height profiles are presented in Figs. 2(a)–2(c). The thickness of BP is about 32.6 nm with β-Ga_2O_3 flakes of 123.5 nm. Moreover, AFM image indicates that a vertical heterojunction can be fabricated by directly covering the multilayer BP on the β-Ga_2O_3 flake. Fig. 2(d) shows the Raman spectrum of BP, β-Ga_2O_3 and the BP/β-Ga_2O_3 heterojunction (overlapped region) on the Si/SiO_2 substrate. Three characteristic peaks of BP located at 362, 440, and 467 cm^{-1}, corresponding to A_g^1, B_{2g}, and A_g^2 vibration modes, respectively[17]. The peak about 200 cm^{-1} corresponds to the A_g^3 vibration mode of the β-Ga_2O_3[2]. The observed peaks are consistent with previously reported data. The peaks of both BP and β-Ga_2O_3 can be observed in the overlapped region without significant changes comparing to non-overlapped regions. These results confirm the good quality of the flakes in the heterostructure and neither materials have obvious destruction after exfoliation and device fabrication. Fig. 2(e) shows the SEM image (left) of BP/β-Ga_2O_3 heterojunction, which reveals the material surfaces are smooth. Element mappings (right) indicate that Ga atoms and P atoms are evenly distributed in the heterostructure device.

To demonstrate the fabricated BP/β-Ga_2O_3 PN heterojunction is available, the electrical properties of the as-fabricated BP/β-Ga_2O_3 heterojunction FETs as well as the individual BP and β-Ga_2O_3 devices are exhibited in Fig. 3. Fig. 3(a) shows the source–drain current I_{ds} as a function of back gate voltage (V_{bg}) at a fixed source–drain bias voltage (V_{ds} = 0.1 V) for the BP FET. Meanwhile, the I_{ds}–V_{ds} curves under different V_{bg} (ranging from –60 to 60 V with steps of 30 V) are presented in the inset of Fig. 3(a). The device shows a typical p-type ambipolar transistor, which is consistent with previous reports[16]. Similarly, Fig. 3(b) shows I_{ds}–V_{bg} curve at a fixed V_{ds} = 5 V for the β-Ga_2O_3 FET, the I_{ds}–V_{ds} curves under different V_{bg} (ranging from –80 to 80 V with steps of 40 V) are presented in the inset of Fig. 3(b). The device exhibits an obvious n-type semiconducting transistor behavior. According to the linear I_{ds}–V_{ds} curves shown in the inset of Figs. 3(a) and 3(b), there is a good ohmic contact between the materials and the electrodes. The circuit schematic diagram of the PN heterojunction is shown in the inset of Fig. 3(c). As shown in Figs. 3(c) and 3(d), the I_{ds}–V_{ds} curve and semi-log plot for the BP/β-Ga_2O_3 heterojunction exhibit a clear rectifying behavior with a rectification ratio about 10^7, reverse current around pA and threshold voltage near 1.0 V. The rectification ratio is defined as the ratio of the forward/reverse current, which is usually used to check the degree of rectification[41]. These strong rectifying behaviors reveal that there is a good van der Waals PN heterojunction formed between p-type BP and n-type β-Ga_2O_3.

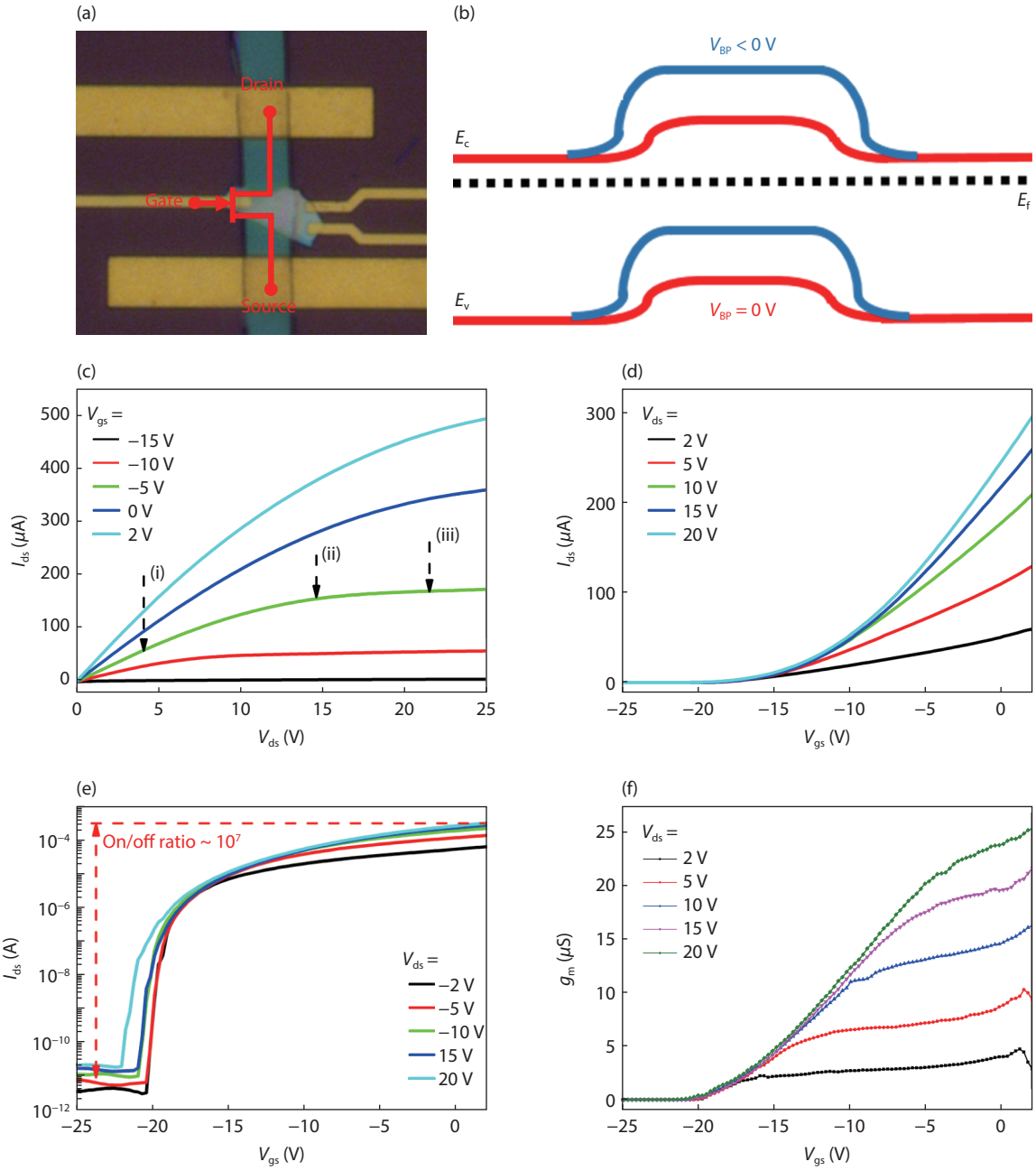

Fig. 4. (Color online) (a) Circuit schematic diagram and optical image of the BP/β-Ga_2O_3 JFET. (b) Band diagram of β-Ga_2O_3 along the channel length direction. The red and blue curve shows the band bending at zero and negative gate voltage, respectively. (c) Output characteristics (I_{ds}–V_{ds}) of the JFET. V_{gs} ranging from –15 to 2 V under V_{ds} swept from 0 to 25 V. (d) Transfer characteristics (I_{ds}–V_{gs}) of the JFET. V_{ds} ranging from 2 to 20 V under V_{gs} swept from –25 to 2 V. (e) Semi-log plot of the transfer characteristics of the JFET. It shows a high on/off ratio beyond 10^7. (f) Transconductance curves (estimated from transfer curves of (d)) of BP/β-Ga_2O_3 JFET as function of V_{gs} with V_{ds} sweeping from 2 to 20 V.

To further investigate the properties of the BP/β-Ga_2O_3 PN heterojunction, BP/β-Ga_2O_3 JFET devices were fabricated. The circuit schematic diagram and optical image of the BP/β-Ga_2O_3 JFET are shown in the Fig. 4(a). Using the p-type BP as the gate and n-type β-Ga_2O_3 as the channel, a PN heterojunction formed at the BP/β-Ga_2O_3 vdW interface. According to the operational mechanism of JFETs, the diode characteristics within the gate-channel PN junction are crucial in determining the final JFET characteristics[9]. Fig. 4(b) shows the band diagram of β-Ga_2O_3 along the channel length direction at different V_{gs}. When V_{gs} = 0 V, the energy band of β-Ga_2O_3 is expected to shift upwards slightly (red lines) due to Fermi level alignment. If a negative voltage is applied on BP (V_{gs} < 0 V), the β-Ga_2O_3 energy band will go further upward (blue lines) and the channel will be fully depleted. Therefore, the JFET switched on or off can be modulated effectively by gate voltage on BP. Output characteristics (I_{ds}–V_{ds}) of the JFET with different V_{gs} (ranging from –15 to 2 V) are shown in Fig. 4(c) and obvious I_{ds} saturation are observed. According to a previous report[38], the output curves were divided into three stages for typical JFET characteristics: (i) linear, (ii) pinch-off, and (iii) saturation. When V_{ds} was small, I_{ds}–V_{ds} curves displayed a linear function. As V_{ds} increased further, the channel reached to pinch-off state with a knee V_{ds} about 15 V. At last, I_{ds} appeared as a saturation phenomenon (also called constant current) where I_{ds} remained constant as V_{ds}

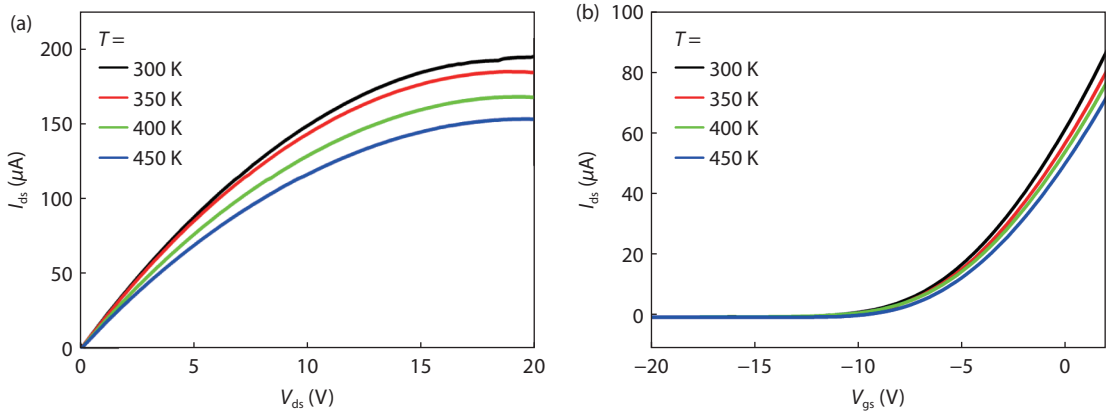

Fig. 5. (Color online) (a) Output characteristics curves of the BP/β-Ga_2O_3 JFET under different temperatures (ranging from 300 to 450 K with steps of 50 K) at V_{gs} = 1 V. (b) Transfer characteristics curves of the BP/β-Ga_2O_3 JFET under different temperatures (ranging from 300 to 450 K with steps of 50 K) at V_{ds} = 10 V.

continuously increased. Figs. 4(d) and 4(e) show the typical transfer characteristics (I_{ds}–V_{gs}) and semi-log plot of the JFET at various V_{ds} (ranging from 2 to 20 V). When a negative voltage was applied on BP, the depletion region of the gate-channel PN junction widened and the channel of β-Ga_2O_3 became synchronously narrower, resulting in the channel resistance increased and the I_{ds} decreased. The threshold voltage was about –20 V. Thus the source-drain current was switched on (demonstrating n-type transport) when V_{gs} > –20 V and switched off when V_{gs} < –20 V, corresponding to effectively switched on/off of the JFET. The ON/OFF ratio is beyond 10^7 indicating high heterojunction interface quality with low trap density. Fig. 4(f) shows the transconductance plots at various V_{ds} extracting from Fig. 4(d). The maximum transconductance (g_m) is of 25.3 μS. The field-effect mobility is one of the most important parameters for both MOSFET and JFET, which can be directly estimated from transfer characteristics. The g_m can be calculated by the following equation[9]:

$$g_m = \frac{dI_D}{dV_{GS}} = \frac{qN_d\mu tW}{L},$$

where N_d is the unintentional doping carrier density; μ is the field-effect mobility; q is an electronic charge; and L, t, and W are the length, thickness and width of the channel, respectively. So, the field-effect mobility μ can be calculated as follows,

$$\mu = \frac{Lg_m}{qN_dtW}.$$

The maximum field-effect mobility μ_{max} of the BP/β-Ga_2O_3 JFET is 14.7 $cm^2V^{-1}s^{-1}$ when g_m is 25.3 μS. The subthreshold swing (SS) is another important parameter for describing the performance of transistors. To achieve lower power consumption and higher integration, it is essential to minimize the SS. The theoretical limit of JFET SS value is 60 mV/dec due to the lack of complicated dielectric engineering. To investigate the performance of BP/β-Ga_2O_3 JFET in the subthreshold regime, the minimum SS of 260 mV/dec is reached when V_{ds} = 20 V and V_{gs} = –21 V. Reducing the thickness and effective carrier concentration of β-Ga_2O_3 nanosheets will be available for further improving the SS of BP/β-Ga_2O_3 JFET devices.

To understand the working regimes of the BP/β-Ga_2O_3 JFET device at different temperatures, temperature-dependent electrical characteristics tests were carried out. The typical output and transfer characteristics at various temperatures (ranging from 300 to 450 K with steps of 50 K) are presented in Figs. 5(a) and 5(b), respectively. Obviously, the JFET characteristics were well maintained. According to the output characteristics curves of the BP/β-Ga_2O_3 JFET device under various temperatures (Fig. 5(a)), obvious I_{ds} saturation and three stages for typical JFET characteristics (linear, pinch-off and saturation) are observed. While, the I_{ds} decreased with the increasing temperature probably because of lower carrier mobility and enhanced phonon scattering. As shown in Fig. 5(b), transfer characteristics curves of the BP/β-Ga_2O_3 JFET device under different temperatures demonstrate typical JFET characteristics that V_{gs} control I_{ds}. The pinch-off voltage is about –18 V, I_{ds} is switched off when V_{gs} < –18 V and switched on when V_{gs} > –18 V, corresponding to effectively switched off/on of the JFET.

4. Conclusion

Herein, we have successfully fabricated vdW heterojunction JFET devices based on multilayer p-type BP as the gate and n-type β-Ga_2O_3 flakes as the channel by mechanically exfoliated methods. The BP/β-Ga_2O_3 heterojunctions possess clean interfaces. Furthermore, the BP/β-Ga_2O_3 PN junction devices show clear rectification characteristics of a high rectifying ratio about 10^7 and low reverse current around pA. These strongly rectifying behaviors demonstrate that a good van der Waals PN heterojunction formed between p-type BP and n-type β-Ga_2O_3. More importantly, the fabricated JFET devices show excellent n-channel JFET properties such as high I_{ds} on/off ratio of 10^7, low gate leakage current around pA, high g_m of 25.3 μS and I_{DSS} of 16.5 μA/μm. In addition, the devices have a pinch-off voltage of –20 V and a minimum subthreshold swing of 260 mV/dec. The temperature-dependent electrical characteristics of JFET devices are also discussed. The JFET characteristics are well maintained although the I_{ds} decreased with the increasing temperature. This work paves the way for vdW heterojunctions based on 2D semiconductors whose application will realize high-performance JFET devices.

Acknowledgements

This work was supported by the National Natural Sci-

ence Foundation of China (Grant No. 61922082, 61875223, 61927813) and the Natural Science Foundation of Jiangsu Province (Grant No. BK20191195). The support from the Vacuum Interconnected Nanotech Workstation (Nano-X) of Suzhou Institute of Nano-tech and Nano-bionics (SINANO), Chinese Academy of Sciences, is also acknowledged.

References

[1] Orita M, Ohta H, Hirano M, et al. Deep-ultraviolet transparent conductive β-Ga_2O_3 thin films. Appl Phys Lett, 2000, 77, 4166
[2] Pearton S J, Yang J C, Cary P H, et al. A review of Ga_2O_3 materials, processing, and devices. Appl Phys Rev, 2018, 5, 011301
[3] Zhou H, Zhang J C, Zhang C F, et al. A review of the most recent progresses of state-of-art gallium oxide power devices. J Semicond, 2019, 40, 011803
[4] Dong H, Xue H W, He Q M, et al. Progress of power field effect transistor based on ultra-wide bandgap Ga_2O_3 semiconductor material. J Semicond, 2019, 40, 011802
[5] Higashiwaki M, Sasaki K, Murakami H, et al. Recent progress in Ga_2O_3 power devices. Semicond Sci Technol, 2016, 31, 034001
[6] Hwang W S, Verma A, Peelaers H, et al. High-voltage field effect transistors with wide-bandgap β-Ga_2O_3 nanomembranes. Appl Phys Lett, 2014, 104, 203111
[7] Ahn S, Ren F, Kim J, et al. Effect of front and back gates on β-Ga_2O_3 nano-belt field-effect transistors. Appl Phys Lett, 2016, 109, 062102
[8] Kim J, Mastro M A, Tadjer M J, et al. Heterostructure WSe_2–Ga_2O_3 junction field-effect transistor for low-dimensional high-power electronics. ACS Appl Mater Interfaces, 2018, 10, 29724
[9] Guo J, Wang L Y, Yu Y W, et al. SnSe/MoS_2 van der Waals heterostructure junction field-effect transistors with nearly ideal subthreshold slope. Adv Mater, 2019, 31, 1902962
[10] Hajnal Z, Miró J, Kiss G, et al. Role of oxygen vacancy defect states in then-type conduction of β-Ga_2O_3. J Appl Phys, 1999, 86, 3792
[11] Barman S K, Huda M N. Mechanism behind the easy exfoliation of Ga_2O_3 ultra-thin film along (100) surface. Phys Status Solidi RRL, 2019, 13, 1800554
[12] Liu Y, Huang Y, Duan X F. Van der Waals integration before and beyond two-dimensional materials. Nature, 2019, 567, 323
[13] Yan X D, Esqueda I S, Ma J H, et al. High breakdown electric field in β-Ga_2O_3/graphene vertical barristor heterostructure. Appl Phys Lett, 2018, 112, 032101
[14] Kim J, Kim J H. Monolithically integrated enhancement-mode and depletion-mode β-Ga_2O_3 MESFETs with graphene-gate architectures and their logic applications. ACS Appl Mater Interfaces, 2020, 12, 7310
[15] Kim J, Mastro M A, Tadjer M J, et al. Quasi-two-dimensional h-BN/β-Ga_2O_3 heterostructure metal–insulator–semiconductor field-effect transistor. ACS Appl Mater Interfaces, 2017, 9, 21322
[16] Li L K, Yu Y J, Ye G J, et al. Black phosphorus field-effect transistors. Nat Nanotechnol, 2014, 9, 372
[17] Liu H, Neal A T, Zhu Z, et al. Phosphorene: an unexplored 2D semiconductor with a high hole mobility. ACS Nano, 2014, 8, 4033
[18] Xia F N, Wang H, Jia Y C. Rediscovering black phosphorus as an anisotropic layered material for optoelectronics and electronics. Nat Commun, 2014, 5, 4458
[19] Zhou Z Q, Cui Y, Tan P H, et al. Optical and electrical properties of two-dimensional anisotropic materials. J Semicond, 2019, 40, 061001
[20] Xu Y J, Shi Z, Shi X Y, et al. Recent progress in black phosphorus and black-phosphorus-analogue materials: Properties, synthesis and applications. Nanoscale, 2019, 11, 14491
[21] Qiao J S, Kong X H, Hu Z X, et al. High-mobility transport anisotropy and linear dichroism in few-layer black phosphorus. Nat Commun, 2014, 5, 4475
[22] Deng B C, Tran V, Xie Y J, et al. Efficient electrical control of thin-film black phosphorus bandgap. Nat Commun, 2017, 8, 14474
[23] Xu Y J, Shi X Y, Zhang Y S, et al. Epitaxial nucleation and lateral growth of high-crystalline black phosphorus films on silicon. Nat Commun, 2020, 11, 1330
[24] Youngblood N, Chen C, Koester S J, et al. Waveguide-integrated black phosphorus photodetector with high responsivity and low dark current. Nat Photonics, 2015, 9, 247
[25] Chen X L, Lu X B, Deng B C, et al. Widely tunable black phosphorus mid-infrared photodetector. Nat Commun, 2017, 8, 1672
[26] Zhu W K, Wei X, Yan F G, et al. Broadband polarized photodetector based on p-BP/n-ReS_2 heterojunction. J Semicond, 2019, 40, 092001
[27] Batmunkh M, Bat-Erdene M, Shapter J G. Black phosphorus: Synthesis and application for solar cells. Adv Energy Mater, 2018, 8, 1701832
[28] Yang Y, Gao J, Zhang Z, et al. Black phosphorus based photocathodes in wideband bifacial dye-sensitized solar cells. Adv Mater, 2016, 28, 8937
[29] Muduli S K, Varrla E, Kulkarni S A, et al. 2D black phosphorous nanosheets as a hole transporting material in perovskite solar cells. J Power Sources, 2017, 371, 156
[30] Ricciardulli A G, Blom P W M. Solution-processable 2D materials applied in light-emitting diodes and solar cells. Adv Mater Technol, 2020, 1900972
[31] Ge X X, Xia Z H, Guo S J. Recent advances on black phosphorus for biomedicine and biosensing. Adv Funct Mater, 2019, 29, 1900318
[32] Wu G, Wu X J, Xu Y J, et al. High-performance hierarchical black-phosphorous-based soft electrochemical actuators in bioinspired applications. Adv Mater, 2019, 31, 1806492
[33] Tao W, Kong N, Ji X Y, et al. Emerging two-dimensional monoelemental materials (Xenes) for biomedical applications. Chem Soc Rev, 2019, 48, 2891
[34] Qiu M, Wang D, Liang W Y, et al. Novel concept of the smart NIR-light-controlled drug release of black phosphorus nanostructure for cancer therapy. Proc Natl Acad Sci USA, 2018, 115, 501
[35] Xu Y J, Yuan J, Zhang K, et al. Field-induced n-doping of black phosphorus for CMOS compatible 2D logic electronics with high electron mobility. Adv Funct Mater, 2017, 27, 1702211
[36] Lv W, Fu X, Luo X, et al. Multistate logic inverter based on black phosphorus/SnSeS heterostructure. Adv Electron Mater, 2019, 5, 1800416
[37] Jeon P J, Lee Y T, Lim J Y, et al. Black phosphorus-zinc oxide nanomaterial heterojunction for p–n diode and junction field-effect transistor. Nano Lett, 2016, 16, 1293
[38] Lim J Y, Kim M, Jeong Y, et al. Van der Waals junction field effect transistors with both n- and p-channel transition metal dichalcogenides. npj 2D Mater Appl, 2018, 2, 37
[39] Wang J H, Liu D N, Huang H, et al. In-plane black phosphorus/dicobalt phosphide heterostructure for efficient electrocatalysis. Angew Chem Int Ed, 2018, 57, 2600
[40] Zheng Y, Yu Z H, Ou H H, et al. Black phosphorus and polymeric carbon nitride heterostructure for photoinduced molecular oxygen activation. Adv Funct Mater, 2018, 28, 1705407
[41] He Q Y, Liu Y, Tan C L, et al. Quest for p-type two-dimensional semiconductors. ACS Nano, 2019, 13, 12294
[42] Deng Y X, Luo Z, Conrad N J, et al. Black phosphorus-monolayer MoS_2 van der Waals heterojunction p–n diode. ACS Nano, 2014, 8, 8292
[43] Lv Q, Yan F G, Mori N, et al. Interlayer band-to-band tunneling and negative differential resistance in van der Waals BP/InSe field-effect transistors. Adv Funct Mater, 2020, 30, 1910713